KU LEUVEN

Department of Mechanical Engineering
Energy Systems Integration & Modeling Group

Energy Systems Integration & Modeling Group Working Paper Series
No. ESIM2020-03

An improved treatment of operating reserves in generation expansion planning models

Sebastian Gonzato, Kenneth Bruninx, Erik Delarue

Last update: 25th February 2020

An improved treatment of operating reserves in generation expansion planning models

Sebastian Gonzato*†, Kenneth Bruninx*† and Erik Delarue*†
* Department of Mechanical Engineering, KU Leuven, Leuven
† Energy Ville, Genk

***Abstract*—Energy system optimisation (ESOM) and generation expansion planning (GEP) models are often used to study energy transition pathways. These typically entail an increased penetration of variable renewable energy sources (VRES), which can lead to increased operating reserve requirements due to their associated forecast uncertainty. Representing this effect has previously been tackled using either stochastic programming techniques or deterministic GEPs which use heuristics to size reserves while ignoring their activation cost. In this paper, we propose a novel GEP formulation which determines operating reserve requirements using a second order cone (SOC) constraint. This formulation approximates the solution of a stochastic GEP by accounting for reserve activation costs without resorting to scenario based methods. A case study on the Belgian system indicates possible cost savings of 70 M€ (0.9%) and less bias towards installing peaking technologies to satisfy reserve requirements compared to a deterministic GEP. The sensitivity of the results to the assumption of normality of forecast errors and temporal detail is also investigated. Two final case studies on the value of emergency measures and improving forecast uncertainties illustrate the benefits of accounting for reserve activation costs and appropriate reserve sizing.**

***Index Terms*—Energy System Optimisation Models, Generation Expansion Planning Models, Operating Reserves, Uncertainty**

I. Introduction

Energy system optimisation models (ESOMs) suggest possible pathways for the energy transition by determining minimum cost investments to satisfy energy demands, typically subject to a carbon emissions target [1]. Meeting these carbon emission targets often requires an increased penetration of variable renewable energy sources (VRES) in the power sector. At these high penetrations, forecast uncertainties may require increased operating reserves. Due to their large technological scope however, increases in forecast uncertainty are often neglected, or simple rules for sizing operating reserves are used. Generation expansion planning (GEP) models are similar to ESOMs but focus solely on the power sector, hence more operational detail can be included. Poncelet [2] included unit commitment (UC) style constraints in a GEP and found that of these the addition of reserve requirements had one of the greatest impacts on system cost and the capacity mix, a finding confirmed by Palmintier [3]. This motivates the pursuit of novel GEP formulations which improve the representation of short term forecast uncertainty. This paper does so with the additional objective of integrating these improvements in an ESOM, hence computational burden and simplicity are also key motivators.

Stochastic programming allows representing short term uncertainty explicitly in GEP models. Pineda et al. [4] investigate the effects of jointly optimising the deterministic day-ahead and stochastic balancing (or reserve activation) markets in a two-stage stochastic GEP, illustrating that doing so is cost effective. While stochastic programming techniques lead to an optimal trade-off between reliability and total costs, this trade-off typically incurs a high computational burden, though this can be mitigated using dedicated optimisation techniques such as progressive hedging [5]–[7]. The quality of the solution is also highly dependent on the quality of the scenario generation and reduction techniques used [8], [9]. Applying these techniques is made all the more difficult in a GEP model since the impact of the uncertainty on, e.g., wind power forecasts depends on the installed capacities (which are decision variables), and hence one needs to characterise each source of uncertainty separately and use a set of scenarios for each of them. With multiple sources of uncertainty, the number of scenarios required to obtain a stable solution may be prohibitively high. Given this, research in the field has focused on dedicated optimisation techniques [5], [6], [10].

Other attempts to address forecast uncertainty and variability in GEP models have pursued a deterministic framework, typically by adding operating reserve requirements [2]. These reserves are sized proportionally to the capacity or availability of the sources of uncertainty (e.g. VRES generation) and then summed together [2], [3], [11]–[13]. This approach is similar to robust interval optimisation [14], and consequently the computed reserves are overly conservative: by adding the reserve requirements due to different sources of uncertainty instead of convoluting the underlying distributions, the likelihood of extreme events is overestimated. In addition, the expected costs associated with activating (i.e. using) these

S. Gonzato is supported via the Energy Transition Funds project EPOC 2030-2050 organised by the FPS economy, S.M.E.s, Self-employed and Energy. K. Bruninx is a post-doctoral research fellow of the Research Foundation - Flanders (FWO) at the University of Leuven and EnergyVille. His work was funded under postdoctoral mandates no. 12J3317N, sponsored by the Flemish Institute for Technological Research (VITO), and no. 12J3320N, sponsored by FWO.

978-1-7281-2822-1/20/$31.00

Reserve sizing	Reserve activation	Scenario based	Model	Section
Proportional	×	×	*P-D*	Section II-A
Approximate Convolution	×	×	*AC-D*	Section II-E
Approximate Convolution	✓	×	*AC-PR*	Section II-C
Exact Convolution	✓	×	*EC-PR*	Section II-D
Implicit	✓	✓	*I-S*	Section II-B

TABLE I: Summary of models GEP models studied in this paper ordered in terms of improving operating reserve representation and computational complexity. Note that *D* stands for Deterministic and *PR* for Probabilistic Reserves.

reserves[1] is typically not accounted for, leading to a bias towards technologies with low investment but high operational costs [15].

Krishnan et al. [16] attempt to avoid overly conservative reserve requirements in a GEP model by assuming normally distributed uncertainty in demand and wind generation forecasts. The reserves requirements are a multiple of the standard deviation of the net load forecast uncertainty, calculated using a convolution which is approximated via a square root approximation. Adapting this approximation for more sources of uncertainty is non-trivial and its accuracy is not reported. Moreover, reserve activation costs are not considered.

There is therefore a gap in the literature for a GEP model which includes reserve requirements (as in [2], [3], [11], [12]) sized using the net load forecast uncertainty (as in [16]) and whose activation costs are accounted for (as in [4]). In order to integrate these improvements into ESOMs, this should be done without resorting to stochastic programming so as to limit the increase in computational complexity. This work attempts to fill that gap by presenting a GEP formulation which sizes reserves using a second order cone (SOC) relaxation to convolve uncorrelated normal distributions, thus avoiding overly conservative reserve requirements. By accounting for the expected cost of activating said reserves using a method inspired by Bruninx and Delarue [15], the GEP model provides near cost-optimal technology mixes and so approximates the solution of an equivalent stochastic GEP.

The rest of this paper is structured as follows. The novel and other GEP model formulations are presented in Section II. These are then compared and contrasted in Section III, with the benefits of considering reserve activation illustrated using two case studies in Section III-D. Section IV concludes.

II. GEP MODEL FORMULATIONS

The GEP models outlined in this section were deliberately kept simple (e.g. by omitting any inter temporal constraints) to focus on the effect of operating reserve requirements and the costs involved. First, a typical deterministic GEP with reserves is described in Section II-A. An equivalent stochastic model is presented in Section II-B. Modification of this last model leads to the novel GEP in Section II-C. To isolate the impact of (1) approximating the convolution of normal distributions using SOC constraints and (2) accounting for reserve activation costs, two additional models are presented in Sections II-D and II-E. All models use the representative periods approach to temporal representation [17] though the period index is not shown for the sake of brevity. A summary of the different models is presented in Table I.

[1]In this paper the term reserve activation is used to refer to real time balancing.

A. Deterministic GEP with proportional reserve constraints P-D

P-D is a linear, deterministic greenfield GEP with reserve requirements:

$$\min \sum_{g\in G} c_g^{fix} + \sum_{\forall t}\left(\sum_{g\in G} c_{g,t}^{gen} + VOLL\cdot ls_t\right) \quad (1)$$

$$\text{s.t.} \quad c_g^{fix} = FC_g \cdot k_g \qquad g\in G \quad (2)$$

$$c_{g,t}^{gen} = AC_g \cdot q_{g,t} \qquad g\in G,\ \forall t \quad (3)$$

$$\sum_{g\in G} q_{g,t} = D_t - ls_t \qquad \forall t \quad (4)$$

$$q_{g,t} + r_{g,t}^{+} \le AF_g \cdot k_g \qquad g\in G_D,\ \forall t \quad (5)$$

$$q_{g,t} + r_{g,t}^{-} \ge 0 \qquad g\in G_D,\ \forall t \quad (6)$$

$$q_{g,t} + \chi_{g,t} = RP_{g,t}\cdot k_g \qquad g\in G_R,\ \forall t \quad (7)$$

$$r_{g,t}^{+} \le \chi_{g,t} \qquad g\in G_R,\ \forall t \quad (8)$$

$$r_{g,t}^{-} \le RP_{g,t}\cdot k_g \qquad g\in G_R,\ \forall t \quad (9)$$

$$\sum_{g\in G_R,\forall t} q_{g,t}\cdot \ge \phi\cdot\sum_{\forall t}(D_t - ls_t) \quad (10)$$

$$\sigma_t = \sum_{g\in G_R}\sigma_g\cdot k_g\cdot RP_{g,t} + \sigma_D\cdot D_t \quad \forall t \quad (11)$$

$$D_t^{+} = RC\cdot\sigma_t \qquad \forall t \quad (12)$$

$$D_t^{-} = RC\cdot\sigma_t \qquad \forall t \quad (13)$$

$$D_t^{+} \ge \sum_{g\in G} r_{g,t}^{+} \qquad \forall t \quad (14)$$

$$D_t^{-} \ge \sum_{g\in G} r_{g,t}^{-} \qquad \forall t \quad (15)$$

The objective function (1) is expressed as the sum of fixed (c_g^{fix}) and generation costs ($c_{g,t}^{gen}$). The fixed cost c_g^{fix} of a technology g its the annualised fixed unit cost FC_g times installed capacity k_g. The generation cost of a technology g at a particular time step $c_{g,t}^{gen}$ is defined as the product of the average generation cost AC_g and the generation of that technology at that time step, $q_{g,t}$. The cost of emergency measure deployment (modelled here as load shedding) is incorporated by multiplying the value of lost load, $VOLL$, with the load shed ls_t.

Constraint (4) is the power balance, which ensures that the electricity generated is equal to the electricity consumed minus load shedding at all time steps. Constraint (5) limits generation $q_{g,t}$ and scheduled upward reserves $r_{g,t}^{+}$ of dispatchable technologies $G_D \subset G$ to the installed capacity derated by an availability factor AF_g. Constraint (6) similarly

limits generation and scheduled downward reserves $r^{-}_{g,t}$. Renewable generators (i.e. VRES) $G_R \subset G$ respect the equality Constraint (7), which states that the power generated plus curtailment is equal to the installed capacity multiplied by the normalised generation profile $RP_{g,t}$. Constraints (8) and (9) constrain reserve provision for VRES and Constraint (10) dictates that a fraction ϕ of the net total energy consumed $\sum_t D_t - ls_t$ must be produced by VRES.

Constraints (11) - (15) size and allocate operating reserves in the model. Constraint (11) approximates the standard deviation of the uncertain net load σ_t by summing the standard deviations of the seperate sources of forecast uncertainty. This σ_t is then used to size reserves similarly to [2], [3], [11], [13]. Constraints (12) - (13) set the reserves to cover a multiple RC of this standard deviation e.g. if RC = 3 then 99.9% of the uncertainty is covered by the reserves, while (12) - (13) allocates these reserves.

It is not typical to formulate operating reserve requirements by constraints (11) - (15), but doing so highlights two key points while being equivalent to more typical formulations [2], [3]. The first is that σ_t is conservatively approximated in Eq. (11) leading to overly larger reserve requirements. Assuming uncorrelated normally distributed uncertainties, the correct expression for σ_t would given by Eq. (16):

$$(\sigma_t)^2 = \sum_{g \in G_R} (\sigma_g \cdot k_g \cdot RP_{g,t})^2 + (\sigma_D \cdot D_t)^2 \quad \forall t \qquad (16)$$

The second point is that by including reserve constraints, this model is implicitly modelling an operating reserve market[2]. However, no balancing costs are taken into account in the objective function. The technologies providing reserves may therefore be sub optimal, and as a consequence so may the capacity mix. This reserve representation therefore resembles a robust interval optimisation approach [14].

B. Stochastic GEP I-S

The stochastic GEP below is inspired by Pineda et al. [4].

$$\min \sum_{g \in G} c^{fix}_g + \sum_{\forall t} \Bigg(\sum_{g \in G} c^{gen}_{g,t} + VOLL \cdot ls_t + \sum_{g \in G} c^{res,act} + c^{res,shed}_t \Bigg) \qquad (17)$$

$$\text{s.t.} \quad (2) - (10)$$

$$D^S_{s,t} = \sum_{g \in G_R} \alpha^{G_R}_{g,s,t} \cdot k_g \cdot RP_{g,t} + \alpha^D_{s,t} \cdot D_t \quad s \in S,\ \forall t \quad (18)$$

$$D^S_{s,t} = \sum_{g \in G} r^S_{g,s,t} + rs^S_{s,t} \quad s \in S,\ \forall t \quad (19)$$

$$rs^S_{s,t} \geq 0 \quad s \in S,\ \forall t \quad (20)$$

$$r^{+}_{g,t} \geq r^S_{g,s,t} \quad g \in G,\ s \in S,\ \forall t \quad (21)$$

$$r^{-}_{g,t} \geq -r^S_{g,s,t} \quad g \in G,\ s \in S,\ \forall t \quad (22)$$

$$c^{res,act}_{g,t} = \sum_{s \in S} P^S_s \cdot AC_g \cdot r^S_{g,s,t} \quad g \in G,\ \forall t \quad (23)$$

$$c^{res,shed}_t = \sum_{s \in S} P^S_s \cdot VOLL \cdot rs^S_{s,t} \quad \forall t \quad (24)$$

Equation (18) defines the deviation from the expected net load ($\sum_{g \in G} q_{g,t} - D_t - ls_t$) in a particular scenario s as the sum of the predicted renewable generator power $k_g \cdot RP_{g,t}$ and load D_t multiplied respectively by the factors $\alpha^{G_R}_{g,s,t}$ and $\alpha^D_{s,t}$, which are obtained by sampling from a forecast error distribution. Constraint (19) requires that redispatching actions in that scenario mitigate this deviation using dispatchable or renewable generators $r^S_{g,s,t}$ or by shedding load ($rs^S_{s,t}$). Redispatching actions are limited by the scheduled reserves through constraints (21) and (22).

The expected cost of redispatching for a technology g at timestep t (which is analogous to the cost of activating reserves for that technology) is defined by Eq. (23) as the redispatch measure $r^S_{g,s,t}$ multiplied by the average cost of generation of that technology AC_g weighted by the probability of that scenario occurring P^S_s. The expected cost of load shedding in the balancing stage[3] is similarly defined by Eq. (24) as the product of load shedding in a scenario s, the value of lost load $VOLL$ and the probability P^S_s.

Stochastic GEP formulations typically limit the first stage variables (i.e. variables not indexed by scenarios) to investment decisions, in this case just k_g [5], [6], [10]. The above formulation was chosen however since it allows for direct comparison with the other models, though some discrepancies remain and are discussed in Section V-A. It can be thought of as modelling both the day-ahead energy-reserve and real-time balancing markets when optimising investments [4]. This improvement on *P-D* comes at the cost of an increasing number of variables and constraints due to the inclusion of scenarios. The number of scenarios $|S|$ required to reach a stable solution also increases with the sources of uncertainty: if 5 scenarios are required per source, then for 3 sources $|S| = 125$, for 4 sources $|S| = 625$. If integrated into an ESOM, the *I-S* formulation would likely have to be solved using dedicated optimisation techniques.

C. Probabilistic GEP with approximate convolved reserve requirements and activation costs AC-PR

The *AC-PR* formulation below is similar to *I-S* with two notable differences. First, instead of sampling from individual forecast uncertainty distributions, these distributions are convolved within the optimisation problem to obtain the distribution of the net load forecast uncertainty. Inspired by common practice with chance constraints, this is done using the SOC constraint (25) to sum the variances of the individual distributions. The second difference is that sampling before solving the GEP problem is replaced by a technique inspired by [15], in which the distribution is uniformly discretised into intervals. The probability of the real time net load deviation exceeding the lower bound of these intervals is then used to

[2]An abstraction is made of whether these flexibility requirements in the form of operating reserves are provided by market participants or the transmission system operator.

[3]From henceforth this will be referred to as reserve shedding.

determine the probability, hence expected cost, of activating reserves to address the resulting imbalance (see Fig. 1).

$$\min \quad (17)$$

$$\text{s.t.} \quad (2)-(10)$$

$$(\sigma_t)^2 \geq \sum_{g\in G_R} \left(\sigma_g \cdot k_g \cdot RP_{g,t}\right)^2 + \left(\sigma_D \cdot D_t\right)^2 \quad \forall t \quad (25)$$

$$\sigma_t \leq \sum_{g\in G_R} \sigma_g \cdot k_g \cdot RP_{g,t} + \sigma_D \cdot D_t \quad \forall t \quad (26)$$

$$D_t^{L^+} = \frac{RC}{|L^+|} \cdot \sigma_t \quad l \in L^+,\ \forall t \quad (27)$$

$$D_t^{L^-} = \frac{RC}{|L^-|} \cdot \sigma_t \quad l \in L^-,\ \forall t \quad (28)$$

$$D_{l,t}^{L^+} = \sum_{g\in G} r_{g,l,t}^{L^+} + rs_{l,t}^{L^+} \quad l \in L^+,\ \forall t \quad (29)$$

$$D_{l,t}^{L^-} = \sum_{g\in G} r_{g,l,t}^{L^-} \quad l \in L^-,\ \forall t \quad (30)$$

$$r_{g,t}^{+} = \sum_{l\in L^+} r_{g,l,t}^{L^+} \quad g \in G,\ \forall t \quad (31)$$

$$r_{g,t}^{-} = \sum_{l\in L^-} r_{g,l,t}^{L^-} \quad g \in G,\ \forall t \quad (32)$$

$$c_{g,t}^{res,act} = \sum_{l\in L^+} P^{L^+} \cdot AC_g \cdot r_{r,l,t}^{L^+} \quad (33)$$

$$- \sum_{l\in L^-} P^{L^-} \cdot AC_g \cdot r_{r,l,t}^{L^-} \quad g \in G,\ \forall t \quad (34)$$

$$c^{res,shed} = \sum_{l\in L^+} P^{L^+} \cdot VOLL \cdot rs_{l,t}^{L^+} \quad \forall t \quad (35)$$

The second order cone constraint (25) is used to convolve normally distributed forecast errors[4]. By specifying a reserve coverage RC and a set of upward reserve levels L^+ with $|L^+|$ elements, the uniform size of the reserve levels $D_{l,t}^{L^+}$ and $D_{l,t}^{L^-}$ is defined by constraints (27) - (28). Constraints (29) - (30) specify that reserve requirements must be met by generators or reserve shedding[5]. Constraints (31) - (32) define the total amount of reserves scheduled by a technology while Eq. (34) - (35) are analogous to (23) - (24).

Equation (25) must be binding to allow for a correct representation of the net load forecast uncertainty distribution. If the costs associated with reserve provision, activation and shedding ($c_{g,t}^{res,prov}$, $c_{g,t}^{res,act}$ and $c_{g,t}^{res,shed}$ respectively) were positive for all timesteps then this would be ensured. The negative term in Eq. (34) associated with activating downward reserves means that a binding SOC constraint cannot be ensured, and so this is only an approximate convolution. For this reason Eq. (26) was added to the model to limit this distortion, while model *EC-PR* was introduced to compare the solution if the convolution was exact. A graphical illustration of this approximation for 2 sources of uncertainty is shown in Fig. 2.

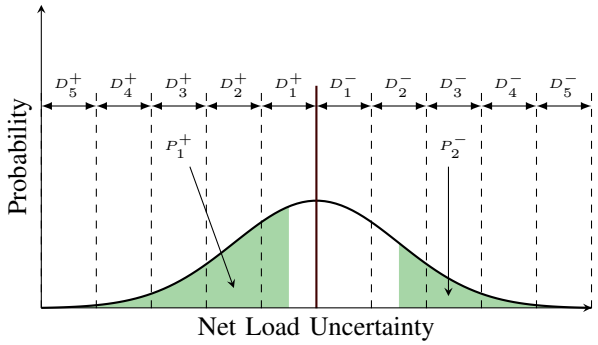

Fig. 1: Illustration of how reserve levels are related to the forecast uncertainty. The forecast uncertainty distribution is split up into segments D_l^+ and D_l^- called reserve levels, whose probability of activation is calculated by integrating the distribution up to the midpoint of the reserve level as shown above for D_1^+. This probability is the likelihood that an imbalance will lead to those reserves being used.

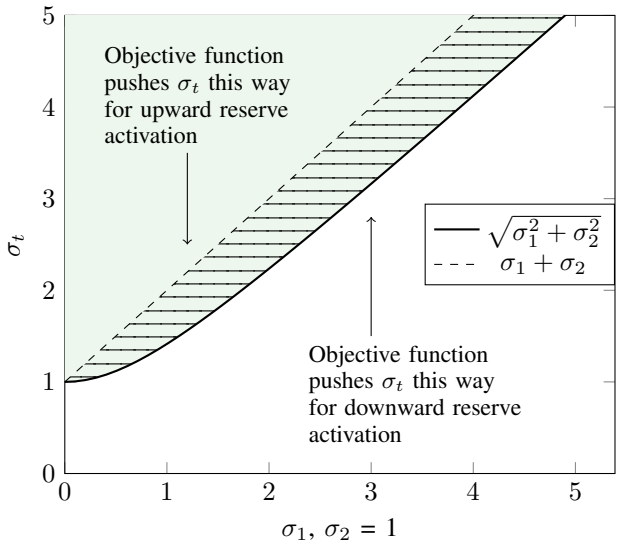

Fig. 2: Bounds on σ_t in the *AC-PR* model. Green area is feasible region given by the SOC constraint (25). Hatcheted area is the feasible region once the linear inequality (26) is imposed.

The advantage of the *AC-PR* model is that the number of constraints is no longer a function of the number of sources of uncertainty as it was with the *I-S* model. Unlike the *I-S* model however, normally distributed and uncorrelated forecast errors must be assumed in order for $P_l^{L^+}$ and $P_l^{L^-}$ to remain parameters. The assumption of uncorrelated distributions is typically correct for forecast errors[6] [18]. The same cannot be said for the assumption of normality [19], [20], an assumption which is checked in Section III-B. This drawback can be mitigated by using distributionally robust techniques [21].

[4]Assuming normally distributed VRES forecast errors can sometimes lead to un-physical values. A discussion of this is presented in Section V-B

[5]Load shedding in the balancing stage of the stochastic model, $rs_{s,t}^{S}$, is analogous to reserve shedding for the *AC-PR* model, $rs_{s,t}^{L^+}$. For this reason, both are referred to as reserve shedding in this paper.

[6]This is not the same as saying that the actual time series are uncorrelated.

D. Deterministic GEP with exact convolution and probabilistic reserves EC-PR

Since the novel *AC-PR* model can only approximate the convolution of uncorrelated normal distributions, the *EC-PR* model is used to compare the result were this convolution to be exact. This is done by adding an equality constraint to the *AC-PR* model to replace Eq. (25) - (26). The resulting problem is non-convex but was solved to global optimality using Gurobi 9 [22]. This formulation is impractical as it proved to be intractable for more than 8 representative days (see Section III-C) but it is useful as a reference case.

$$\min \quad (17)$$

$$\text{s.t.} \quad (2)-(10), \quad (25)-(35), \quad (16)$$

E. Deterministic GEP with approximate convolved reserves AC-D

The novel model *AC-PR* has two improvements on the *P-D* model - reduced reserve requirements and accounting for reserve activation costs. To distinguish the effects these two modifications have on the results, the *AC-D* model is introduced in which no activation costs are considered and reserve shedding is not permitted. In effect this is a chance constrained GEP with upward and downward reliability set by $\Pr\left(\sum_{g\in G} r^{+}_{g,t} \geq \mathcal{N}(0,\sigma_t)\right) \geq RC$ and $\Pr\left(\sum_{g\in G} r^{-}_{g,t} \geq \mathcal{N}(0,\sigma_t)\right) \geq RC$ respectively.

$$\min \quad (1)$$

$$\text{s.t.} \quad (2)-(10), \quad (25)-(35)$$

III. Case studies

This section analyses the characteristics of the novel GEP formulation. In Section III-A the various models are compared in terms of cost, capacity mix, computation times, and reserve scheduling and activation. Robustness to different sources of uncertainty and the level of temporal information is investigated in Section III-B and Section III-C. Two additional case studies are presented in Section III-D to illustrate the advantages of the *AC-PR* model.

A non-exhaustive list of data inputs and assumptions for the case studies in this section is presented below.

- Demand data D_t was obtained from the ENTSO-E transparency platform [23] for the Belgian system in 2018.
- Onshore wind and solar photovoltaic (PV) power generation were similarly obtained through ENTSO-E [23] for Belgium and normalised by installed nameplate capacity to obtain renewable generation profiles $RP_{g,t}$.
- A RES penetration target of $\phi = 50\%$ was used.
- A VOLL of 10,000 €/MWh was used.
- 8 representative days and their weights were selected using the method described in [17] unless otherwise stated.
- Key technology data is given in Table II.

g	FC_g [M€/GW/year]	AC_g [€/MWh]	AF_g [-]
Base	180	36.0	0.85
Mid	101	53.0	0.85
Peak	69	76.0	0.85
Wind	146	0.0	
PV	92.0	0.0	

TABLE II: Key technology data. Fixed and average generation costs (FC_g and AC_g) were obtained from [11]. Availability factors AF_g where assumed to be 0.85 for dispatchable generators while time dependent VRES generation profiles $RP_{g,t}$ (not shown) where obtained from the ENTSO-E transparency platform [23].

- Standard deviation values used for VRES forecast uncertainty were $\sigma_{Wind} = 0.033$ and $\sigma_{PV} = 0.025$ such that three standard deviations corresponded to the variable renewable forecast error reserve requirements used by NREL's Resource Planning Model [13].
- Standard deviation value used for load forecast uncertainty was $\sigma_D = 0.028$, obtained from a statistical analysis of historical data of the Belgian power system in 2018.
- In the *I-S* simulations, $5^3 = 125$ uniformly sampled scenarios were used to keep computation times acceptably low while reaching in-and-out-of-sample stability (see Fig. 3a).
- An out-of-sample analysis[7] is conducted to verify the total costs obtained from the GEP simulations.
- Scenarios were obtained by sampling uniformly from the normal distributions described above, with 5 scenarios per distribution
- $|L^+| = |L^-| = 15$ for the *AC-PR* model since $|L^+| = |L^-| > 10$ led to in-and-out-of-sample stability.
- $RC = 3$ was used and hence 99.9% of the forecast uncertainty was covered by reserves in the *AC-PR* simulations.

The Julia code for all case studies can be found at: `https://gitlab.kuleuven.be/u0128861/operating-reserves-in-GEPs`.

A. Impact of improved reserve sizing and including reserve activation costs on the GEP solution

In this section the 5 models are compared in terms of cost, capacity mix, reserve scheduling and activation and computation times. Fig. 3a shows the trend in total costs for the different models. Comparing *P-D* and *AC-D* reveals that the reduced reserve requirements lead to a decrease in total costs of approximately 30 M€. These are primarily due to decreased investment costs resulting from the ability to shed reserves (see Table III). The decrease in in sample costs observed when comparing *AC-D* with *AC-PR*, *EC-PR* and *I-S* models is similarly due to a decrease in capital expenditure, this time due to the ability of the latter models to deploy reserve shedding when this is economical. The *AC-PR*, *EC-PR* and *I-S* models are within 0.05% of the out of sample results,

[7]For the out-of-sample analysis the capacities resulting from the simulations were fixed and then the models repeatedly simulated for various scenarios until the 95% confidence interval was less than 0.01% of the total costs or more than 10,000 scenarios were run [18].

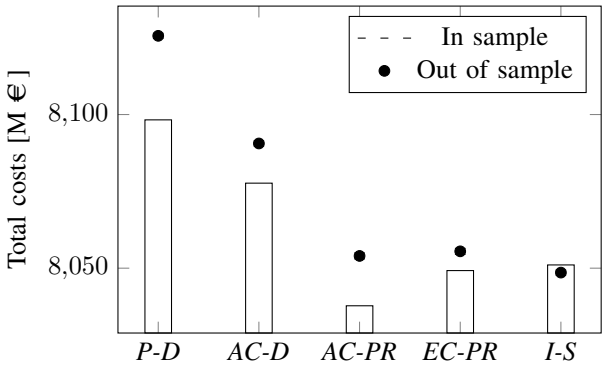

(a) Total in and out of sample costs. Models which consider reserve activation costs lead to lower total costs.

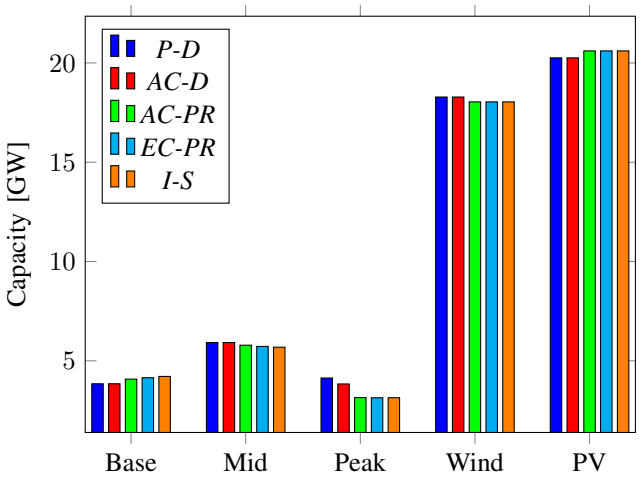

(b) Capacity mix. Models which consider reserve activation costs are install less Peak and Mid capacity.

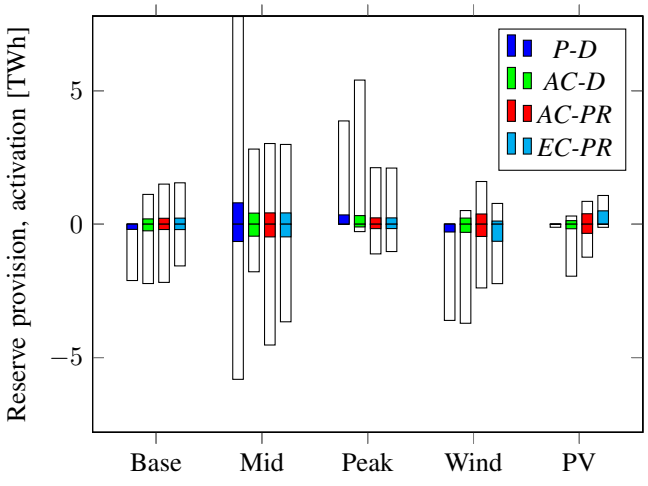

(c) Reserve provision (empty bars) and expected reserve activation (filled bars). Models which don't consider reserve activation schedule Peak technology almost exclusively for upward reserves. *I-S* model is not shown here since discrepancy in model formulation leads to significant increase in amount of scheduled reserves compared to other models (see Section V-A).

Fig. 3: Comparison of costs, installed capacity and (expected) reserve provision for models *P-D*, *AC-D*, *AC-PR*, *EC-PR* and *I-S*.

with remaining discrepancies explained by the difference in expected energy not served (EENS) values due to the different representations of uncertainty.

As expected, *AC-PR* underestimates total costs since it overestimates the cost savings possible from activating downwards reserves by 16 M€. This underestimation is dwarfed however by the 72 M€ saved compared to *P-D*. In addition, the capacity mix of *AC-PR* is similar to that of the other models which consider balancing costs more accurately, *EC-PR* and *I-S* (see Fig. 3b). Since they account for activation costs, these models install less peak capacity (which is cheap to install but expensive to run) compared to the deterministic *P-D* and *AC-D* models. Fig. 3c illustrates this behaviour quite clearly. Peak capacity is scheduled to provide upward reserves almost exclusively for the deterministic models whereas it is also scheduled for downward reserves for the probabilistic reserve models. Note that the total scheduled upward reserves is also greatly reduced.

In this study, we did not consider any technical requirements for the reserve providers (e.g., ramping limits, maximum activation times) in order to isolate the effect of reserve sizing and reserve activation in GEP models and to avoid any bias towards specific assumptions on the flexibility of different technologies or the requirements for reserve providers [2]. Adding such constraints may lead to, e.g., more peak capacity installed in the *AC-PR*, *EC-PR* and *I-S* simulations.

Model	Total costs [M€]	Fixed costs [M€]	Max load + reserve shedding [GW]	EENS [GWh]
P-D	8126 (8098)	6108	0	0 (0)
AC-D	8091 (8078)	6088	0	0.2 (0)
AC-PR	8054 (8038)	6066	0.53	1.5 (1.1)
EC-PR	8056 (8049)	6072	0.53	1.7 (1.1)
I-S	8049 (8051)	6080	0.75	0.8 (0.9)

TABLE III: Summary of key results from simulations for 8 representative days, with bracketed numbers indicating in sample results. The maximum expected load shedding value gives an indication of the reduction in capacity achieved by economic shedding of reserves. Much of the cost savings can be explained by reductions in fixed investment costs, which are achieved either through improved reserve sizing, the ability to shed reserves, or both.

B. Robustness of AC-PR *model to the assumption of normally distributed uncertainty*

To test the assumption of normality's robustness against uncertainty, an out of sample analysis was conducted using five different distributions (as inspired by [24]), with the results reported in Table IV. Since the model used to run the out of sample analysis is running "at the limit" of its capabilities, it is unsurprising that the total costs are very sensitive to the EENS. The Student t distribution leads to such high costs because it has "fatter" tails than a normal distribution and hence a greater chance of load needing to be shed in real time. This effect may motivate the inclusion of a planning reserve margin (PRM) to deal with low probability, high impact events. However, a PRM is subject to the same issue as the operating reserves in *P-D*, namely that the cost of operating technologies is not considered [25].

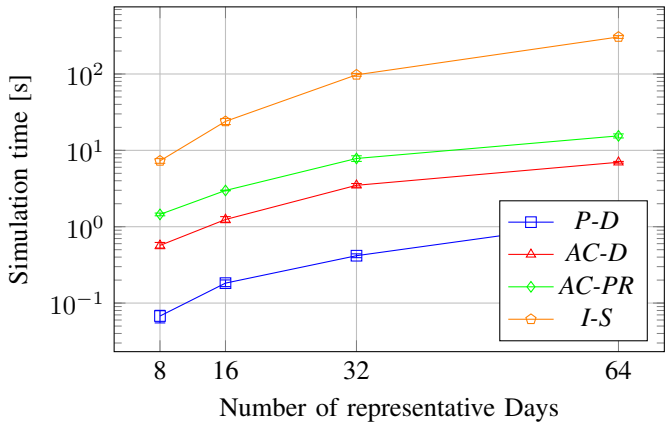

(a) Simulation times as a function of the number of representative days. *AC-PR* is a bit less than an order of magnitude faster than *I-S*.

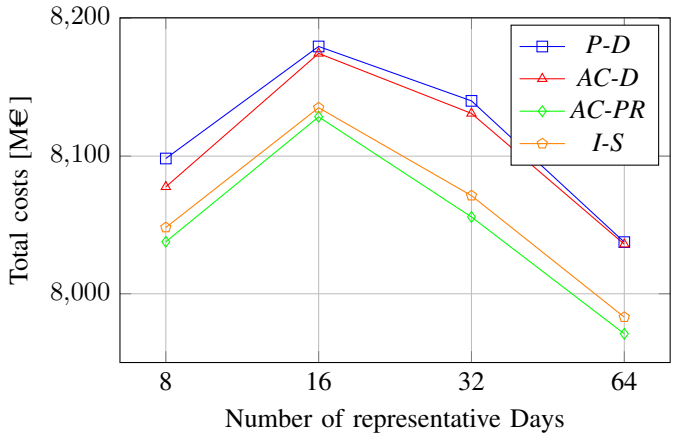

(b) Total costs as a function of the number of representative days. The difference in total costs between models which consider activation costs and those which don't remains in the interval of 0.5-1%.

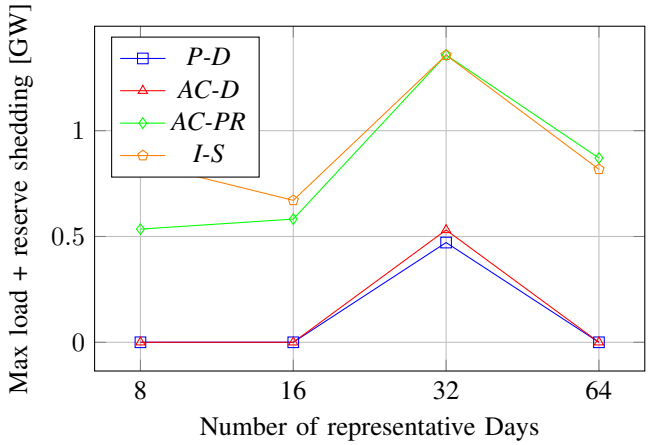

(c) Maximum load shed as a function of the number of representative days. The difference of this value between models which consider activation costs and those which do not is correlated with the difference in total costs ($R^2 = 0.64$ when comparing *P-D* and *AC-PR*).

Fig. 4: Effect of increasing the number of representative days on computation time, the total costs and maximum load shedding. *EC-PR* is not shown since it was not possible to run this simulation for more than 16 representative days.

Distribution	Total Cost [M €]	EENS [GWh]
Reference	8054 (8043)	1.1
Normal with $\sigma_g \times 1.2$	8085 (8039)	4.6
Normal with $\sigma_g \times 0.75$	8052 (8038)	1.4
Left skewed Normal with $\alpha = -5$	8015 (8007)	0.8
Right skewed Normal with $\alpha = 5$	8095 (8069)	2.6
Student t distribution with $\mu = 1$	8704 (8038)	66.6

TABLE IV: Robustness of *AC-PR* model solution to uncertainty. Bracketed values are total costs when EENS costs are subtracted. The heavy tailed Student t distribution leads to the greatest amount of EENS and hence the greatest increase in costs.

C. Sensitivity of results to the number of representative days

Fig. 4a shows the computation times of the various models. The *AC-PR* model can be solved just under an order of magnitude faster than the *I-S* model, though still slower than *P-D* and *AC-D*. The difference between the *AC-PR* and *I-S* models increases if the time taken to build the model is taken into account, though this was not included since it is specific to the particular implementation of the optimisation problem.

Most of the results discussed so far have been limited to simulations with only 8 representative days (192 hours). While this is quite high compared to the 10 - 50 timeslices typically used in ESOMs [26], there could be important interactions between the level of temporal detail and short term uncertainty. For example, the advantage of being able to economically schedule reserve shedding could be negated if more timesteps are considered. Fig. 4b and Fig. 4c show that this is not the case. While there are differences in the results between the number of representative days (see [17] for a discussion on this), for a particular representative day the trends are the same - total costs decrease with improved reserve sizing, and they decrease even more when reserve activation costs are considered. This last trend appears to correlate with the maximum expected load shedding, suggesting that this decrease in costs is due to reduced capacity costs as hypothesised in Section III-A.

D. Benefits of considering reserve activation costs

To illustrate the benefits of considering reserve activation costs, Fig. 5 shows two additional case studies. In Fig. 5a the sensitivity of the models to the cost of deploying emergency measures is investigated. The *AC-PR* model is clearly able to exploit the benefits of reduced emergency measure costs better than the *P-D* and *AC-D* models. In particular, this benefit increasingly outweighs the convolution approximation error as the cost of emergency measures decreases. In Fig. 5b the *AC-PR* and *AC-D* models illustrate how the value of reducing VRES forecast errors might be overestimated by the simpler *P-D* and *AC-D* models.

IV. Conclusions and Future Work

In this paper we presented a novel GEP problem formulation with an improved representation of operating reserves. In Section III-A it was shown that the investment decisions of

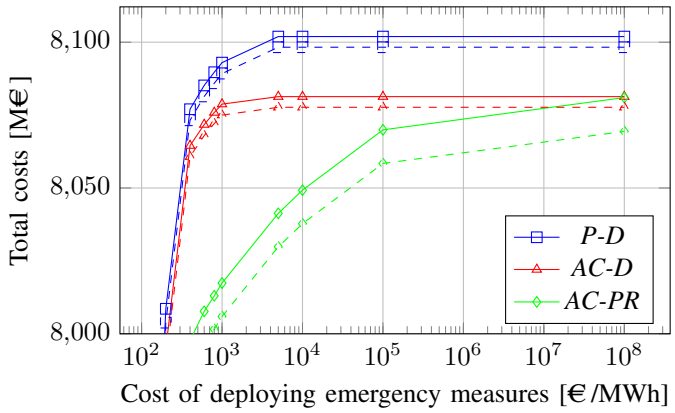

(a) The value of reducing the cost of deploying emergency measures. The *AC-PR* model is able to exploit this flexibility for higher deployment costs than the other two models.

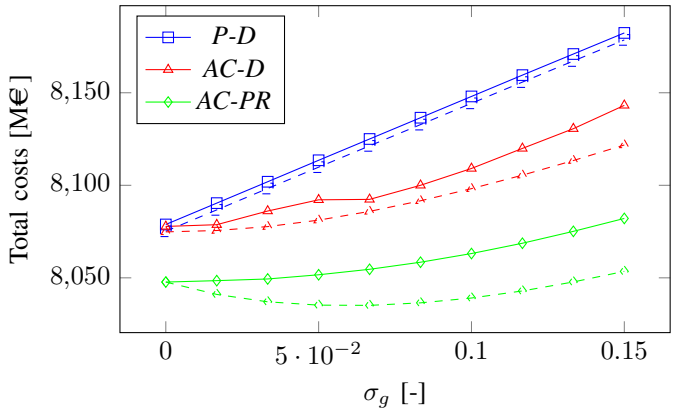

(b) Value of reducing VRES forecast errors in reducing total costs. The *P-D* model predicts a linear increase in costs with a slope proportional to the cost of installing an additional unit of Peak capacity. Note that σ_D was kept constant for these simulations.

Fig. 5: Case studies illustrating the benefits of the *AC-PR* model's ability to approximate *I-S* but faster. Dashed lines are in sample results while solid lines are results obtained when in sample capacities were fed to the *EC-PR* model which was then solved. This was done to approximate the out of sample solution without resorting to the more computationally intensive *I-S* model.

the model were similar to that of an equivalent stochastic model while requiring roughly an order of magnitude less computation time. The results were robust to the temporal detail though sensitive to greater likelihood of extreme scarcity events where load must be shed. Additional case studies on the value of emergency measures and reducing forecasting errors in Section III-D highlighted the benefits of considering reserve activation costs in a GEP formulation.

Given these observations, the *AC-PR* formulation appears suited to situations where operating reserves could drive simulation results (e.g. high VRES systems) and a stochastic model is not possible or required. If this is not the case then the improvements obtained could be obscured by other factors. If applied to a problem then the solution should also be verified by rerunning an operational model with fixed operating reserves to ensure that the downward reserve sizing approximation is tolerable.

Future work could investigate the effect of UC type technical constraints and improved treatment of high impact low probability events on the results. Implementation of the novel GEP formulation into an ESOM could also be considered.

References

[1] D. Connolly, H. Lund, B. V. Mathiesen, and M. Leahy, "A review of computer tools for analysing the integration of renewable energy into various energy systems," *Applied Energy*, vol. 87, no. 4, pp. 1059–1082, 2010. [Online]. Available: http://dx.doi.org/10.1016/j.apenergy.2009.09.026

[2] K. Poncelet, E. Delarue, and W. D'haeseleer, "Unit commitment constraints in long-term planning models: Relevance, pitfalls and the role of assumptions on flexibility," *Applied Energy*, vol. 258, no. August 2019, p. 113843, 2020.

[3] B. Palmintier, "Flexibility in generation planning: Identifying key operating constraints," in *2014 Power Systems Computation Conference*, Aug 2014, pp. 1–7.

[4] S. Pineda, J. M. Morales, and T. K. Boomsma, "Impact of forecast errors on expansion planning of power systems with a renewables target," *European Journal of Operational Research*, vol. 248, no. 3, pp. 1113–1122, 2016.

[5] F. D. Munoz, B. F. Hobbs, and J. P. Watson, "New bounding and decomposition approaches for MILP investment problems: Multi-area transmission and generation planning under policy constraints," *European Journal of Operational Research*, vol. 248, no. 3, pp. 888–898, 2016.

[6] J. Barnett, J. P. Watson, and D. L. Woodruff, "BBPH: Using progressive hedging within branch and bound to solve multi-stage stochastic mixed integer programs," *Operations Research Letters*, vol. 45, no. 1, pp. 34–39, 2017.

[7] J. Bukenberger and B. Palmintier, "Stochastic Generation Capacity Expansion Planning with Approximate Dynamic Programming," *Proceedings of the IEEE Power Engineering Society Transmission and Distribution Conference*, vol. 2018-April, pp. 1–5, 2018.

[8] K. Bruninx and E. Delarue, "Scenario reduction techniques and solution stability for stochastic unit commitment problems," in *2016 IEEE International Energy Conference (ENERGYCON)*, April 2016, pp. 1–7.

[9] Y. Dvorkin, Y. Wang, H. Pandzic, and D. Kirschen, "Comparison of scenario reduction techniques for the stochastic unit commitment," in *2014 IEEE PES General Meeting — Conference Exposition*, July 2014, pp. 1–5.

[10] A. Papavasiliou and S. S. Oren, "Multiarea stochastic unit commitment for high wind penetration in a transmission constrained network," *Operations Research*, vol. 61, no. 3, pp. 578–592, 2013.

[11] A. Van Stiphout, K. De Vos, and G. Deconinck, "The Impact of Operating Reserves on Investment Planning of Renewable Power Systems," *IEEE Transactions on Power Systems*, vol. 32, no. 1, pp. 378–388, 2017.

[12] C. De Jonghe, E. Delarue, R. Belmans, and W. D'haeseleer, "Determining optimal electricity technology mix with high level of wind power penetration," *Applied Energy*, vol. 88, no. 6, pp. 2231–2238, 2011. [Online]. Available: http://dx.doi.org/10.1016/j.apenergy.2010.12.046

[13] T. Mai, C. Barrows, A. Lopez, E. Hale, M. Dyson, and K. Eurek, "Implications of Model Structure and Detail for Utility Planning : Scenario Case Studies Using the Resource Planning Model," National Renewable Energy Laboratory, Denver, Tech. Rep. April, 2015.

[14] S. Boyd, *Convex optimization theory*. Cambridge University Press, 2009, vol. 25, no. 3.

[15] K. Bruninx and E. Delarue, "Endogenous Probabilistic Reserve Sizing and Allocation in Unit Commitment Models: Cost-Effective, Reliable, and Fast," *IEEE Transactions on Power Systems*, vol. 32, no. 4, pp. 2593–2603, 2017.

[16] V. Krishnan, T. Das, E. Ibanez, C. A. Lopez, and J. D. McCalley, "Modeling operational effects of wind generation within national long-term infrastructure planning software," *IEEE Transactions on Power Systems*, vol. 28, no. 2, pp. 1308–1317, 2013.

[17] K. Poncelet, H. Höschle, E. Delarue, A. Virag, and W. D'haeseleer, "Selecting representative days for capturing the implications of integrating intermittent renewables in generation expansion planning problems," *IEEE Transactions on Power Systems*, vol. 32, no. 3, pp. 1936–1948, 2017.

[18] K. Bruninx, "Improved modeling of unit commitment decisions under uncertainty," Ph.D. dissertation, KU Leuven, 2016.

[19] K. Bruninx and E. Delarue, "A statistical description of the error on wind power forecasts for probabilistic reserve sizing," *IEEE Transactions on Sustainable Energy*, vol. 5, no. 3, pp. 995–1002, 2014.

[20] A. Fabbri, T. G. San Román, J. R. Abbad, and V. H. Méndez Quezada, "Assessment of the cost associated with wind generation prediction errors in a liberalized electricity market," *IEEE Transactions on Power Systems*, vol. 20, no. 3, pp. 1440–1446, 2005.

[21] Y. Zhang, S. Shen, and J. L. Mathieu, "Distributionally Robust Chance-Constrained Optimal Power Flow with Uncertain Renewables and Uncertain Reserves Provided by Loads," *IEEE Transactions on Power Systems*, vol. 32, no. 2, pp. 1378–1388, 2017.

[22] L. Gurobi Optimization, "Gurobi optimizer reference manual," 2020. [Online]. Available: http://www.gurobi.com

[23] "Entso-e transparency platform," https://transparency.entsoe.eu/, accessed: 2019-09-06.

[24] J.-F. Toubeau, Z. De Greve, P. Goderniaux, F. Vallee, and K. Bruninx, "Chance-Constrained Scheduling of Underground Pumped Hydro Energy Storage in Presence of Model Uncertainties," *IEEE Transactions on Sustainable Energy*, pp. 1–1, 2019.

[25] T. Mertens, K. Bruninx, K. Poncelet, J. Duerinck, and E. Delarue, "On generation adequacy in long-term power system planning models," Leuven, 2018, working paper.

[26] K. Poncelet, "Long-term energy-system optimization models," Ph.D. dissertation, KU Leuven, 2018.

V. Appendix

A. *Stochastic GEP* I-S *and redispatching*

A key difference between the *I-S* and the other models is that the former is able to re-dispatch downwards (upwards) to deal with a negative (positive) imbalance in real time. This is illustrated in Fig. 6. It is not clear to the authors what this additional degree of freedom has on the behaviour of *I-S* model, though it does appear to make use of it and schedule an order of magnitude more reserves than the other models.

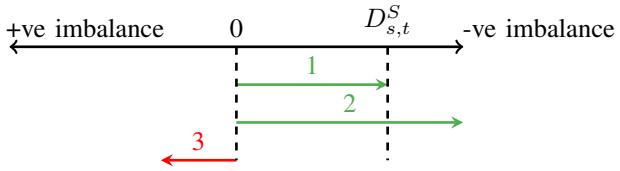

Fig. 6: Illustration of possible redispatch to satisfy an imbalance for the *I-S* model. The negative imbalance realisation $D^S_{s,t}$ can be satisfied by redispatching generators upwards, as shown by arrow 1. Another option would be to redispatch some generators up (arrow 2) but also some down (arrow 3), which when summed up give arrow 1.

B. *Approximating VRES generation profile prediction errors using a normal distribution*

One problem with approximating VRES generation profile $RP_{g,t}$ prediction errors by normal distributions is that while $0 \leq RP_{g,t} \leq 1$, a normally distributed variable can theoretically take on any real value. This problem is partly resolved by artificially cutting off the tails of the normal distribution. There is still the risk that the need for downward reserves is overstated, since a normal could suggest $RP_{g,t}$ values greater than one (see Fig. 7). This was dealt with by separating positive and negative sides of the normal distribution and scaling the standard deviation of the latter such that renewable generation profiles greater 1 are not possible. It should be noted that for 8 representative days this scaling did not change anything since $RC \cdot \sigma_g \cdot RP_{g,t} < 1 \quad \forall g \in G_R, \quad \forall t.$

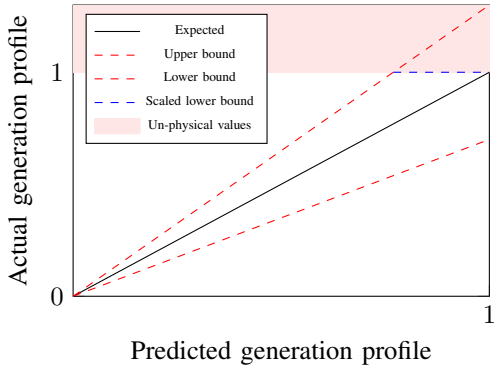

Fig. 7: Illustration of the error when approximating renewable generation profile forecast errors using normal distributions. Scaling resolves problem of having un-physical renewable generation profile values.

KU LEUVEN

Department of Mechanical Engineering
Energy Systems Integration & Modeling Group

On the authors:

Sebastian Gonzato (sebastia.gonzato@kuleuven.be recieved the M.Eng degree in chemical engineering in 2018 from Imperial College London. He is working on generation adequacy within the EPOC 2030-50 project.)

Kenneth Bruninx (kenneth.bruninx@kuleuven.be) received the M.Sc. degree in energy engineering in 2011 and the Ph.D. degree in mechanical engineering in 2016, both from the Univeristy of Leuven (KU Leuven), Belgium. Currently, he is working as a post-doctoral research fellow of the Research Foundation - Flanders (FWO) (grant no. 12J3320N) in the Energy Systems Integration and Modeling Group at the University of Leuven and EnergyVille.

Erik Delarue (erik.delarue@kuleuven.be) received the M.Sc. degree in mechanical engineering in 2005 and the Ph.D. degree in mechanical engineering in 2009, both from the University of Leuven (KU Leuven), Belgium. Currently, he is Assistant Professor at the University of Leuven, leading the Energy Systems Integration and Modeling Group, and active in EnergyVille.

On the research group:

The **Energy Systems Integration & Modeling Group** is part of the division of Applied Mechanics and Energy Conversion (TME) of the Department of Mechanical Engineering of KU Leuven in Belgium. E. Delarue and W. D'haeseleer lead this research group, currently about 15 PhD students and post-doctoral research fellows, dedicated to the modeling of integrated energy systems and markets. This young research group has already gained significant expertise and international recognition in the field. A major strength of this group is its interdisciplinary focus (techno-economic models, link to energy policies and markets). The group is further strongly embedded in EnergyVille, an association of the Flemish research institutes KU Leuven, VITO, imec and UHasselt in the field of sustainable energy and intelligent energy systems. EnergyVille brings research, development, training and industrial innovation together under one name, in close cooperation with local, regional and international partners.